Protein Science (1993), *2*, 1630–1642. Cambridge University Press. Printed in the USA.

Changes in interactions in complexes of hirudin derivatives and human α-thrombin due to different crystal forms

JOHN P. PRIESTLE, JOSEPH RAHUEL, HANS RINK, MICHAEL TONES,[1] AND MARKUS G. GRÜTTER

Department of Biotechnology, Pharmaceuticals Division, Ciba-Geigy Ltd., CH-4002 Basel, Switzerland

(RECEIVED March 16, 1993; ACCEPTED July 7, 1993)

Abstract

The three-dimensional structures of D-Phe-Pro-Arg-chloromethyl ketone-inhibited thrombin in complex with Tyr-63-sulfated hirudin$^{55-65}$ (ternary complex) and of thrombin in complex with the bifunctional inhibitor D-Phe-Pro-Arg-Pro-$(Gly)_4$-hirudin$^{54-65}$ (CGP 50,856, binary complex) have been determined by X-ray crystallography in crystal forms different from those described by Skrzypczak-Jankun et al. (Skrzypczak-Jankun, E., Carperos, V.E., Ravichandran, K.G., & Tulinsky, A., 1991, *J. Mol. Biol. 221*, 1379–1393). In both complexes, the interactions of the C-terminal hirudin segments of the inhibitors binding to the fibrinogen-binding exosite of thrombin are clearly established, including residues 60–64, which are disordered in the earlier crystal form. The interactions of the sulfate group of Tyr-63 in the ternary complex structure explain why natural sulfated hirudin binds with a 10-fold lower K_i than the desulfated recombinant material. In this new crystal form, the autolysis loop of thrombin (residues 146–150), which is disordered in the earlier crystal form, is ordered due to crystal contacts. Interactions between the C-terminal fragment of hirudin and thrombin are not influenced by crystal contacts in this new crystal form, in contrast to the earlier form. In the bifunctional inhibitor–thrombin complex, the peptide bond between Arg-Pro (P1-P1′) seems to be cleaved.

Keywords: blood clotting; crystal artifacts; hirudin; thrombin; X-ray crystallography

The serine proteinase thrombin plays a central role in the blood coagulation process. It activates platelets as well as the blood coagulation factors V, VIII, and XIII that are essential for formation of the blood clot. Moreover, polymerization of fibrin monomers that arise from limited proteolysis of fibrinogen by thrombin forms the basis of this clot (Jackson & Nemerson, 1980). Human α-thrombin consists of two polypeptide chains: an A-chain of 36 residues and a B-chain of 259 residues. There are three disulfide bridges within the B-chain, and one disulfide bridge is formed between the two chains (Bode et al., 1989). The crystal structure of the PPACK–human α-thrombin complex has been determined at 1.9 Å resolution (Bode et al., 1989). The analysis showed that thrombin has the same fold as other trypsinlike serine proteinases. Thrombin differs from trypsin by having several insertion loops, two of which narrow the substrate cleavage site of the enzyme (Bode et al., 1989). The structures of thrombin complexed with PPACK and three other low molecular weight nonpeptidic active-site inhibitors have also been described by Banner and Hadváry (1991). Crystal structures have been solved for human fibrinogen complexed to both human thrombin (Stubbs et al., 1992) and to bovine thrombin (Martin et al., 1992).

Hirudin is the most potent and specific natural thrombin inhibitor (Markwardt, 1970; Walsmann & Markwardt, 1981). It consists of a polypeptide chain of 65 or 66 residues with three disulfide bridges (Bagdy et al., 1976; Dodt et al., 1984, 1985). Its three-dimensional struc-

Reprint requests to: Markus G. Grütter, Department of Biotechnology, Pharmaceuticals Division, Ciba-Geigy Ltd., CH-4002 Basel, Switzerland.

[1] Present address: Ciba-Geigy Ltd., Horsham, England.

Abbreviations: PPACK, D-Phe-Pro-Arg-chloromethyl ketone; DCCI, diisopropylcarbodiimide; DMA, dimethylacetamide; TFA, trifluoroacetic acid; DIPE, diisopropyl ether; HOBt, 1-hydroxyl-benzotriazole; PE, petroleum ether; Pmc, 2,2,5,7,8-pentamethylchromane-6-sulfonyl; ACN, acetonitrile; Fmoc, 9-fluorenyl-methoxycarbonyl; PEG, polyethylene glycol; Trt, triphenylmethyl; tBu, tertiary butyl; DVB, divinylbenzene; HPLC, high-performance liquid chromatography; FAB-MS, fast atom bombardment mass spectroscopy; rms, root mean square. The numbering of thrombin is based on that for chymotrypsin (Bode et al., 1989). The numbering for inhibitor residues corresponds to that of intact hirudin and is preceded by the prefix "h."

ture has been determined by two-dimensional NMR techniques (Clore et al., 1987; Folkers et al., 1989; Haruyama & Wüthrich, 1989). Hirudin forms a compact N-terminal domain (residues 3–49) containing three disulfide bridges between cysteine residues 6 and 14, 16 and 28, and 22 and 39 and a long C-terminal tail composed of residues 50–65 that is disordered in solution. Hirudin inhibits thrombin by forming a tight equimolar complex ($K_i = 10^{-14}$ M; Stone & Hofsteenge, 1986). The unique biochemical properties of the thrombin–hirudin interaction are evident from the structures of the complexes between human α-thrombin and recombinant desulfato-hirudins—variant 1 (Grütter et al., 1990) and variant 2, Lys 47 (Rydel et al., 1990, 1991)—as well as that between bovine thrombin and recombinant desulfato-hirudins variant 1 (Vitali et al., 1992). These structures reveal a mode of binding that had not been observed previously for a proteinase inhibitor. The unique features are: (1) extended areas of hirudin and thrombin are in close contact; (2) the primary specificity pocket of the enzyme is not occupied by any part of hirudin; (3) the three N-terminal amino acids of hirudin bind in the active site and run in a direction that is exactly opposite to that of the substratelike inhibitor PPACK; and (4) the C-terminal fragment of hirudin binds to the fibrinogen-binding exosite of thrombin (Fenton, 1981), making numerous electrostatic as well as hydrophobic interactions that are responsible for the tight binding. A very detailed description of thrombin and its interactions with PPACK and with hirudin has been presented by Bode et al. (1992).

It was clear from the structure of the complex that small synthetic bifunctional inhibitors or hirudin analogs exploiting the active site and the exosite of thrombin, either unlinked or connected by a linker, could be potent thrombin inhibitors and may be useful as therapeutic agents replacing hirudin. Independently, and without detailed structural knowledge, bifunctional inhibitors consisting of an active-site binding part, a linker, and the C-terminal fragment of hirudin have been proposed as potent and specific inhibitors for thrombin (Maraganore et al., 1990; Bourdon et al., 1991). C-terminal fragments of hirudin unlinked to an active-site inhibitor do not inhibit hydrolysis of small synthetic substrates of thrombin (hence K_i cannot be determined) but do bind to the exosite of thrombin (DiMaio et al., 1990) and cause a 50% reduction in plasma clotting time at concentrations around 1 nmol/125 mM of diluted plasma (Maraganore et al., 1989). Linked active-site inhibitors and C-terminal fragments of hirudin do inhibit small synthetic substrate hydrolysis as well as fibrinogen cleavage by thrombin and have K_i values of around 1 nM (Bourdon et al., 1991; Yue et al., 1992). We report here the crystal structures of a ternary complex of thrombin, PPACK, and the C-terminal fragment of hirudin (residues 55–65, sulfated Tyr-63) analyzed at 2.5 Å and the complex of thrombin with an inhibitor made by connecting PPACK to a C-terminal fragment of hirudin (residues 53–65) with the linker Pro-$(Gly)_4$ to 2.2 Å resolution. Skrzypczak-Jankun et al. (1991) have described the structures of two different binary complexes that both crystallize in different crystal forms as compared to the complexes described in this paper. In their hirulog structure, residues 60–64 of hirudin are disordered (residue 65 is missing) as is the autolysis loop of thrombin (residues 146–150). In their binary complex of thrombin with only hirudin residues 55–64, again the autolysis loop is disordered. In contrast, this paper describes the interactions of the hirudin C-terminus with thrombin up to residue 64 as well as a stable conformation for the autolysis loop in the different space group that seems to be governed by crystal packing forces.

Results

The ternary complex

Tyr-63-sulfated hirudin fragment h54-Asp–h65-Gln interactions with thrombin

The hirudin C-terminal peptide fragment h55–h65 interacts with thrombin as the same segment does in the hirudin–thrombin complex. The structure is of interest (1) because of the higher resolution of the diffraction data of the ternary complex crystals as compared to the hirudin–thrombin complex of Grütter et al. (1990), which diffracted only to a resolution of 2.95 Å, (2) because the earlier work was carried out with recombinant desulfatohirudin, and (3) because of the difference in space groups compared to similar work carried out by Skrzypczak-Jankun et al. (1991). In addition to allowing a detailed description of the interactions that are also valid for the hirudin–thrombin complex, interactions brought about by, or lost because of, crystal-packing forces can be examined.

The C-terminal hirudin residues bind to thrombin in the fibrinogen exosite (Grütter et al., 1990; Rydel et al., 1990, 1991; Stubbs et al., 1992). This exosite, extending from the active-site cleft (Fig. 1; Kinemage 1), is flanked by the thrombin surface loops 70–80 on one side and 35–39 on the other side having a high proportion of arginine and lysine residues. Interactions of these basic residues of thrombin with the acidic residues of the C-terminal fragment of hirudin are as follows: Arg-73 forms an ion pair with hAsp-55 of the hirudin fragment. Further polar interactions are between Arg-75 and Arg-77A and the side chain of hGlu-57 of the peptide, also forming an intermolecular ion pair. The peptide amide nitrogen of hGlu-57 also forms a hydrogen bond with the main-chain oxygen of Thr-74 of thrombin. The side chains of residues hGlu-58 and hGlu-61 of the inhibitor interact with the side chains of a symmetry-related thrombin molecule (crystal contact forces). The side chain of residue hGlu-62 is free in solution but nevertheless seems to contribute to general elec-

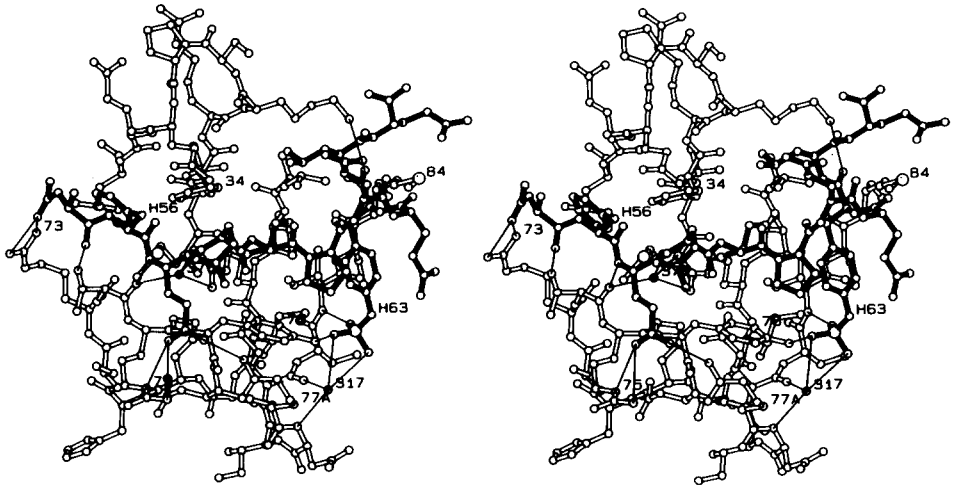

Fig. 1. Entire C-terminal tail of hirudin (solid bonds) of the ternary complex in the exosite of thrombin (open bonds) with thin lines representing potential hydrogen bonds between them (d_{min} = 3.5Å). The sulfate group of hTyr-63 forms two direct and two water-mediated hydrogen bonds with thrombin. The side chain of hGlu-57 forms hydrogen bonds with the side chains of Arg residues 75 and 77A, while that of hGlu 55 forms one with the side chain of Arg-73. Only residues h55 and h57 make main-chain hydrogen bonds with thrombin.

trostatic interactions (Karshikov et al., 1992). In contrast, in the analogous structure of Skrzypczak-Jankun et al. (1991) the side chain of hGlu-57 forms an ion pair with a symmetry-related thrombin molecule while the side chains of hGlu-58 and hGlu-61 are disordered.

Figure 2 shows the electron density around the sulfated hTyr-63 residue. The hTyr-63 in native hirudin is sulfated, and this posttranslational modification causes a 10-fold lower K_i value for natural hirudin as compared to the unsulfated recombinant hirudin (Braun et al., 1988; Dodt et al., 1988, 1990). This has also been found to be true for hirudin C-terminal fragments (Maraganore et al., 1989). Contrary to expectations (Betz et al., 1991a), only hydrogen bonds mediate the interactions between the negatively charged SO_3 group and thrombin. The side chain of Lys-81, the only positively charged group in the vicinity of the sulfate, is disordered, implying that there is no interaction between the two groups. Potential hydrogen bonds are formed between the oxygen atoms of the sulfate group with the amide nitrogen of residue 82, with the O-group of Tyr-76 of thrombin and solvent molecule 317, which is anchored by the amide nitrogen of residue 78 and the carboxyl group of residue 80 of thrombin (Kinemage 1). These results corroborate the interpretations of Skrzypczak-Jankun et al. (1991).

Hydrophobic interactions

The residues hPhe-56, hIle-59, hPro-60, and hLeu-64 form many hydrophobic interactions with the bottom of the exosite canyon (Fig. 3; Kinemage 1). Table 1 lists the corresponding interaction partners of the C-terminal hirudin fragment and thrombin. Thirty-one hydrophobic contacts are made by these residues, and it has been shown by mutagenesis analysis and exchange of the hydrophobic residues what the relative contributions of these interactions are to the stability of the complex.

PPACK interactions with the active site of thrombin

The binding of PPACK is the same as described in the thrombin–PPACK structure of Bode et al. (1989) and Banner and Hadváry (1991). PPACK forms an antiparallel β-strand with Ser-214–Gly-219 of thrombin (Fig. 4; Kinemage 1). D-Phe occupies the S3 site of the enzyme

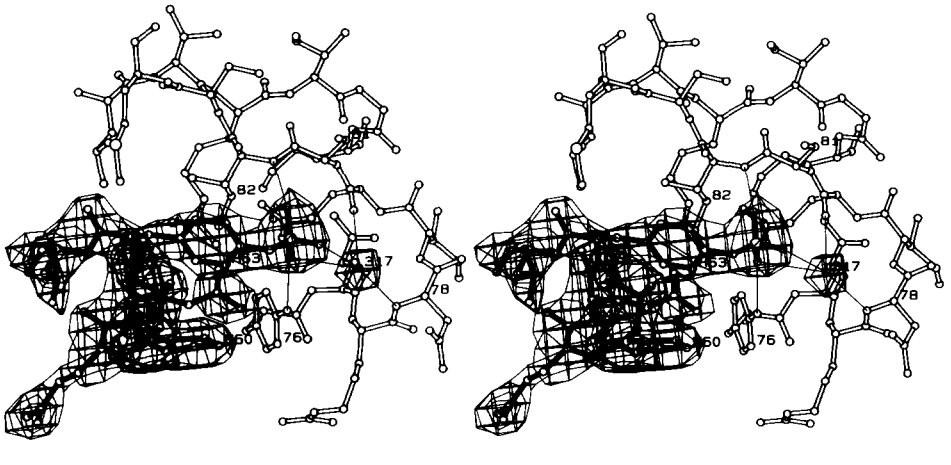

Fig. 2. Electron density around the sulfated Tyr-63 of the ternary complex. Thrombin is shown with open bonds, the C-terminal tail of hirudin with solid bonds. Electron density is from a $2F_o - F_c$, σ_A 2.2 Å Fourier map (Read, 1986) contoured at 1 rms above the mean and is shown only for the hirudin part of the complex and a solvent molecule. Thin lines indicate potential hydrogen bonds between the sulfate group of Tyr-63, solvent molecule 317, and thrombin (d_{min} = 3.5 Å). The side chain for Lys-81 of thrombin is disordered, and only the Cγ atom could be placed with confidence.

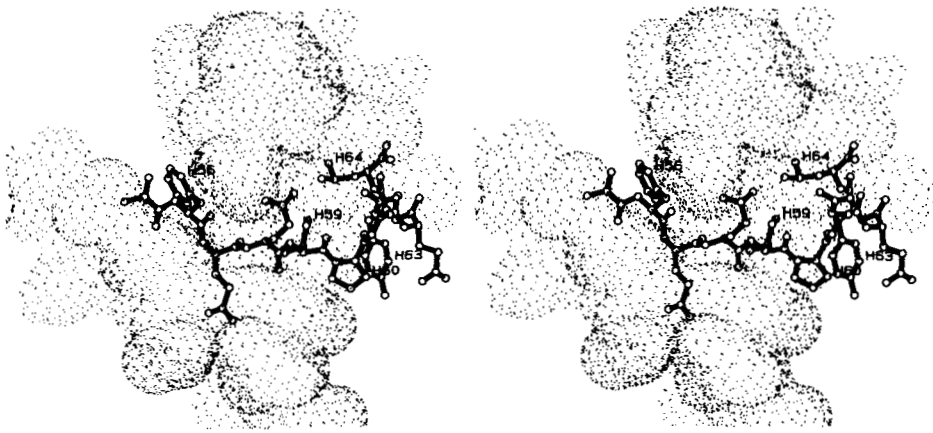

Fig. 3. Entire C-terminal fragment of hirudin (solid bonds) of the ternary complex in the exosite of thrombin with a dot surface at 1.5× the van der Waals radii of the thrombin exosite atoms. The hydrophobic side chains of hPhe-56, hIle-59, and hLeu-64 fit into hydrophobic pockets in the thrombin exosite.

(nomenclature of Schechter & Berger [1967]), Pro the S2 site, and Arg is pointing into the S1 specificity pocket, interacting with Asp-189. Except for hirudin, this is the mode of binding of all natural inhibitors or substrates to serine proteinases in their active sites (Grütter et al., 1989; Bode & Huber, 1991).

The binary complex

The binding of CGP 50,856 to thrombin is very similar to that found in the ternary complex, especially since it seems that the inhibitor is cleaved between Arg-3 and Pro-4. Figure 5 and Kinemage 2 show how the first three res-

Table 1. *Number of contacts (cutoff distance 4.0 Å) between thrombin residues and hirudin-derived inhibitor residues*[a]

Thrombin residue	Hirudin-derived inhibitor residues																		
	H57	Y60A	W60D	E97A	N98	L99	D189	A190	C191	E192	G193	D194	S195	S214	W215	G216	G219	C220	G226	Total
Interactions between inhibitor and active site of thrombin: ternary-binary complex																				
dPhe		1/0		1/1	3/4	3/3									8/8	7/9				23/25
Pro	7/2	3/3	6/0			2/3				0/1				2/2						20/11
Arg	13/**6**						**5/8**	**8/6**	3/3	1/1	1/3	1/1	16/**12**	**6/2**	6/4	6/5	**3/4**	1/1	1/1	71/57
Total	20/8	4/3	6/0	1/1	3/4	5/6	5/8	8/6	3/3	1/2	1/3	1/1	16/12	8/4	14/12	13/14	3/4	1/1	1/1	114/93

Thrombin residue	Hirudin-derived inhibitor residues														
	F34	K36	Q38	L40	L65	R67	R73	T74	R75	Y76	R77A	K81	I82	M84	Total
Interactions between C-terminal tail of hirudin and thrombin: ternary-binary-hirudin complex															
D-55							**5/0/6**	**4/2/4**							9/2/10
F-56	5/5/2		2/**6**/0	1/2/1			3/2/3	3/3/5							14/18/11
E-57			0/1/0					**4/3/1**	**7/6/5**	**8/6/0**	**3/4**/0				22/20/6
E-58			0/3/0							0/0/3					0/3/3
I-59					1/1/1	3/1/3				1/1/0			1/2/0		6/5/4
P-60										7/4/9					7/4/9
E-61															0/0/0
E-62														1/0/0	1/0/0
Y-63		1/3/0			1/2/0					**3**/0/0		3/0/0	**15**/5/3	3/0/1	26/10/4
L-64		3/4/4	0/0/1		1/0/1										4/4/6
Q-65		5/0/0												1/0/0	6/0/0
Total	5/5/2	9/7/4	2/10/1	1/2/1	3/3/2	3/1/3	8/2/9	11/8/10	7/6/5	19/11/12	3/4/0	3/0/0	16/7/3	5/0/1	95/66/53

[a] For the active site, the numbers refer to contacts between thrombin and the ternary complex (PPACK and C-tail of hirudin) and thrombin and the binary complex (CGP 50,856). For the contacts between thrombin and the C-tail of hirudin, the number of contacts for the ternary complex/the binary complex/and hirudin with thrombin are shown. Interactions involving hydrogen bonds are printed in boldface. Interactions involving salt bridges (ion pairs) are printed in boldface and underlined. There are covalent bonds between His-57 and Ser-195 in thrombin and the Arg moiety of PPACK in the ternary complex. Note that hTyr-63 is sulfated in the ternary complex. The side chains for hAsp-55 and hGln-65 of the binary complex could not be unambiguously located.

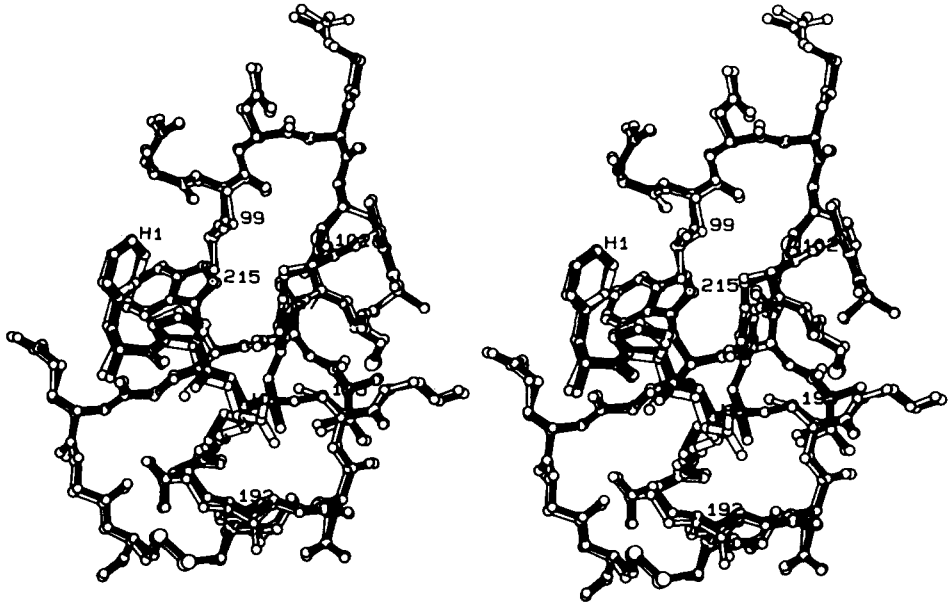

Fig. 4. Superpositioning of the complex of thrombin with CGP 50,856 (open bonds) and the ternary complex (solid bonds). The PPACK moiety of the ternary complex forms covalent bonds with the catalytic residues Ser-195 and His-57 of thrombin.

idues are defined by the electron density in the active site of thrombin. Beyond what was presumably the nitrogen of the subsequent proline residue, no electron density could be found, implying that this actually represented the cleaved inhibitor. This conclusion was also reached by Skrzypczak-Jankun et al. (1991). Qiu et al. (1992) have described the structure of a similar binary complex in which the arginine in the P1 position is replaced by homoarginine and is not cleaved. One clear difference between the active-site inhibitor in the binary and ternary complexes is that it is not covalently bound to the enzyme as in the ternary complex but is held through electrostatic and hydrophobic interactions. Hydrogen bonds between Arg-3 and the thrombin catalytic residues His-57 and Ser-195 replace the covalent bonds formed by PPACK. This difference is manifested by a slight rotation around χ_1 of Ser-195 and a small displacement of the side chain of His-57, as well as a small movement of the carboxylate group at the end of the inhibitor (Fig. 4). This configuration probably represents the last step in hydrolysis before the cleaved substrate leaves the active site (trapped product). The binding of the hirudin carboxyl tail is also very similar to that in the ternary complex. The Pro-$(Gly)_4$ linker has no influence and cannot even be found in the electron density maps (which is also true for the ensuing residues hAsp-53 and hGly-54), implying that this part of the peptide is not specifically interacting with thrombin and is flexible after cleavage (Fig. 6). Again, ion-pair interactions between hGlu-57 of the inhibitor and Arg-75 and Arg-77A of thrombin and hydrophobic interactions involving hPhe-56, hIle-59, hPro-60, and hLeu-64 of the inhibitor make major contributions to binding. The side

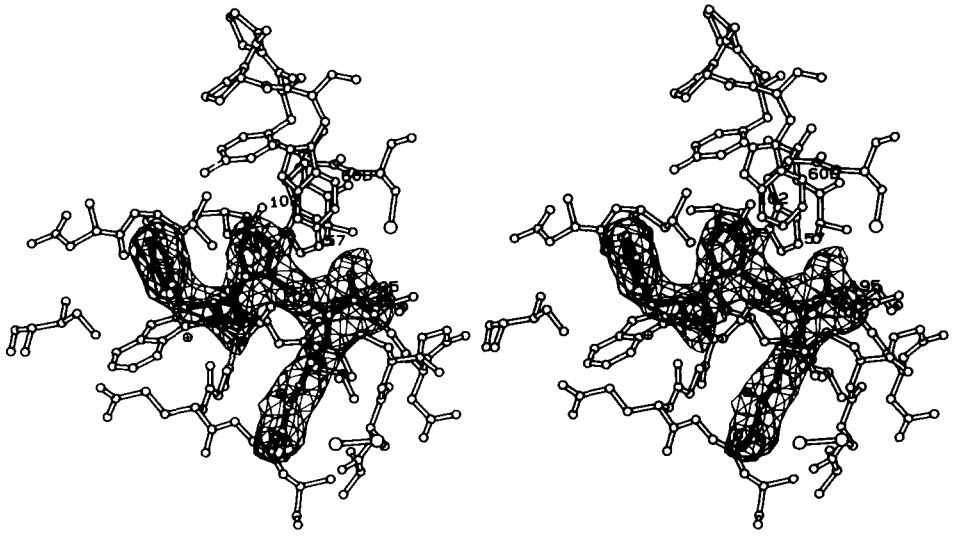

Fig. 5. The active site of thrombin (open bonds) complexed with CGP 50,856 (solid bonds) and electron density for CGP 50,856. All atoms of the inhibitor are clearly defined in the 2.2 $2F_o - F_c$, σ_A Fourier map (Read, 1986) contoured at 1 rms above the mean. The abrupt termination of electron density after the arginine residue in P1 implies that the inhibitor has been cleaved. Solvent molecules are indicated by a circle and a cross.

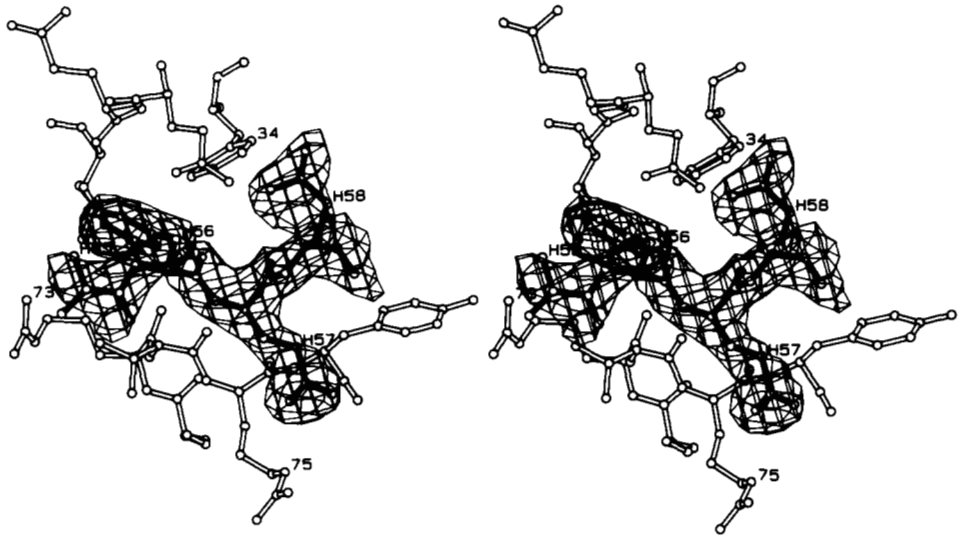

Fig. 6. Residues h55–h58 of CGP 50,856 (solid bonds) with electron density in the exosite of thrombin (open bonds). The 2.2 $2F_o - F_c$, σ_A (Read, 1986) electron density contoured at 1 rms above the mean slowly fades away beyond the amino side of residue h55, implying that the Pro-$(Gly)_4$ linker of CGP 50,856 as well as residue h54 extends out into the solvent in some disorderly fashion after being cleaved. The side chain of h55-Asp could also not be interpreted from the electron density.

chain for hAsp-55 is not well defined by the electron density in the structure of the CGP 50,856–thrombin complex. For a similar structure in a different crystal form, Skrzypczak-Jankun et al. (1991) report that residues hPro-60–hLeu-64 of the hirudin C-terminal fragment (hAsp-55–hLeu-64) are disordered, implying that the contributions to binding by hIle-59, hPro-60, and hLeu-64 are not very large. In the crystal form described here, a neighboring molecule is present that may help keep this segment more rigidly on the thrombin molecule. This illustrates the influence of crystal-packing forces on temperature factors, which are often interpreted in terms of interaction between enzyme and ligand. Having similar structures from different crystal forms available, the danger of overinterpretation of results can be avoided.

Conformational changes of thrombin (the Trp-148 binding loop)

These two structures represent the third crystal form found for thrombin–inhibitor complexes. In all three crystal forms the loop composed of residues 146–150, also called the autolysis loop, possesses a different and, in all three cases, well-defined conformation (Fig. 7; Kinemages 1, 2). This loop contains a five-residue insertion relative to chymotrypsin and was suspected of having high flexibility based on its susceptibility to the proteinases trypsin (Fenton et al., 1977), pancreatic elastase (Kawabata et al., 1985), and cathepsin G or chymotrypsin (Brezniak et al., 1990) and its difference from the canonical binding conformation of inhibitors of serine proteinases (Bode et al., 1989). In the thrombin–hirudin complex, it was believed that the conformation change was due to binding of hirudin (Grütter et al., 1990; Rydel et al., 1991). In the $P2_12_12$ crystals reported here, it is clear that crystal-packing forces are at least partly responsible for the conformation of this loop (Fig. 8). In the monoclinic crystal form of Skrzypczak-Jankun et al. (1991), this loop could not be located and presumably is disordered or flexible. This flexibility could explain why this loop is so easily cleaved by thrombin itself, despite thrombin's high specificity relative to trypsin.

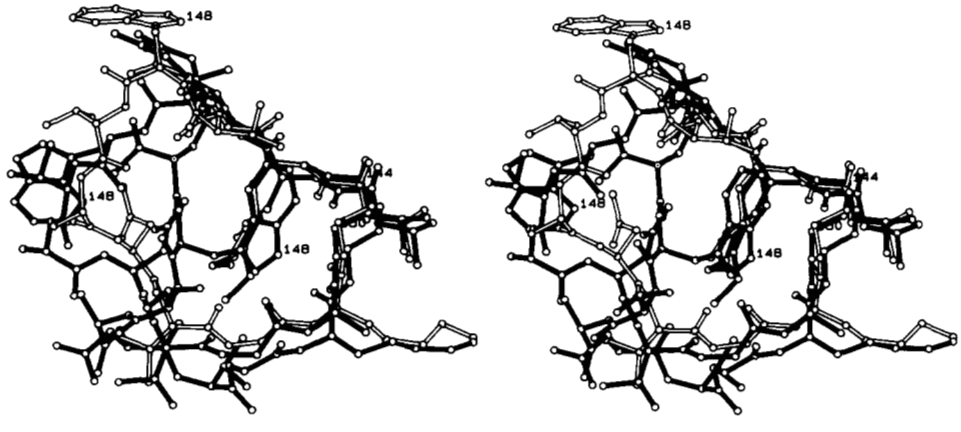

Fig. 7. Conformation of the 149 loop in thrombin as found in three different crystal structures: PPACK-inhibited thrombin (open bonds; Bode et al., 1989), hirudin-inhibited thrombin (striped bonds; Grütter et al., 1990), and CGP 50,856-inhibited thrombin (solid bonds).

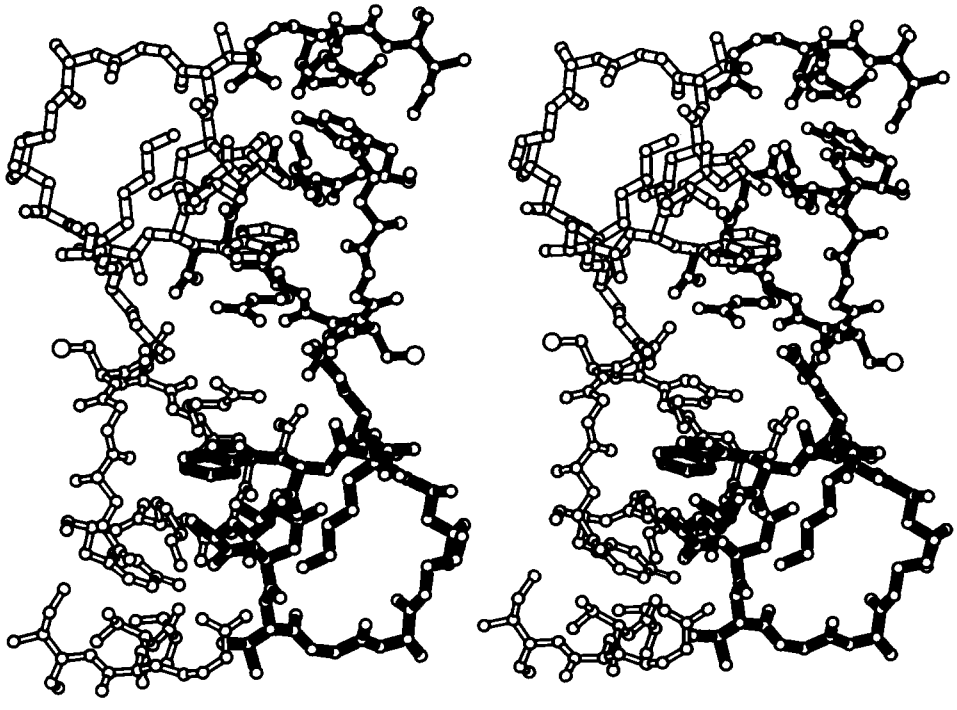

Fig. 8. The interface between two thrombin molecules (open and solid bonds) in the $P2_12_12$ crystallographic unit cell. The twofold axis is perpendicular to the plane of the paper, passing through the center of the picture. The loop 144–150 of thrombin (thicker bonds) makes many intimate contacts with the neighboring molecule.

Discussion

A number of mutants have been made in the C-terminal tail of hirudin to investigate its interactions with thrombin (Braun et al., 1988; Stone et al., 1989; Betz et al., 1991a,b; Yue et al., 1992). These are summarized in Table 2. It is possible to interpret these results with respect to the structure of the complex of hirudin (Rydel et al., 1991) and the structures described in this paper. Looking at the refined temperature factors of the binary complex, it appears that the C-terminal fragment of hirudin, despite the very tight binding constant, remains somewhat flexible after binding to thrombin (Table 3). Its *B*-factors, for both main-chain and side-chain atoms, are approximately 50% higher than those for thrombin, as was also noted by Rydel et al. (1991) for the hirudin–thrombin complex and by Skrzypczak-Jankun et al. (1991) for the hirulog–thrombin complex in their crystal form. In contrast, the *B*-factors of the PPACK moiety are similar or slightly lower than those for thrombin, implying tight, specific binding, especially for the side chains.

The C-terminal fragment of hirudin binds to the fibrinogen-binding groove of thrombin through both electrostatic and hydrophobic interactions (Table 1; see Kinemages 1 and 2). Many positively charged residues line the thrombin groove, yet of the five residues in the C-terminal fragment that are negatively charged only two form salt bridges to thrombin: hAsp-55 with Arg-73 and hGlu-57 with both Arg-75 and Arg-77A. These interactions are the same as those found in the ternary complex of fibrinopeptide A and the C-terminal fragment of hirudin with human α-thrombin (Stubbs et al., 1992). In the

Table 2. *Change in binding energy due to amino acid substitution in the C-terminal fragment of hirudin*

Mutation	ΔΔ (kcal/mol)	Reference
hAsp-53 Ala	−0.05	Betz et al., 1991a
hAsp-55 Asn	+0.57	Betz et al., 1991a
Gly	+0.35	Yue et al., 1992
hPhe-56 Tyr	−0.07	Betz et al., 1991b
Trp	+0.33	Betz et al., 1991b
Ala	+0.45	Betz et al., 1991b
Leu	+2.10	Betz et al., 1991b
Ile	+2.08	Betz et al., 1991b
Val	+2.51	Betz et al., 1991b
Thr	+2.92	Betz et al., 1991b
Gly	+1.91	Yue et al., 1992
hGlu-57 Gln	+1.41	Betz et al., 1991a
Gly	+1.91	Yue et al., 1992
hGlu-58 Gln	+1.27	Betz et al., 1991a
Gly	+0.54	Yue et al., 1992
hIle-59 Gly	+3.38	Yue et al., 1992
hPro-60 Ala	+1.58	Betz et al., 1991b
Gly	+1.36	Betz et al., 1991b
Gly	+1.15	Yue et al., 1992
hGlu-61 Gln	+0.31	Braun et al., 1988
Gly	+0.41	Yue et al., 1992
hGlu-62 Gln	+0.67	Braun et al., 1988
Gly	+0.95	Yue et al., 1992
hTyr-63 Phe	+0.07	Betz et al., 1991b
Ala	+0.53	Betz et al., 1991b
Glu	+0.45	Betz et al., 1991b
Leu	+0.74	Betz et al., 1991b
Val	+1.22	Betz et al., 1991b
Gly	+1.06	Yue et al., 1992
hLeu-64 Gly	+1.15	Yue et al., 1992
hGln-65 Gly	+0.16	Yue et al., 1992

Table 3. *Analysis of temperature (B) factors (in Å²) for the refined structure of the CGP 50,856–thrombin complex*

Moiety or residue	Main chain	Side chain
A. Average main-chain and side-chain *B*-factors for the various parts of the complex[a]		
Thrombin A	32.0 (104)	42.1 (111)
Thrombin B	26.3 (1,028)	35.2 (1,054)
PPACK	30.0 (12)	24.3 (18)
C-tail	44.6 (40)	51.1 (48)
Solvent	43.9 (111)	–
B. Average B-factors for the individual residues of the inhibitor[b]		
hPhe-1	24.5	29.2
hPro-2	27.0	25.0
hArg 3	38.5	19.7
hAsp-55	65.0	92.5[c]
hPhe-56	42.4	46.7
hGlu-57	29.2	48.1
hGlu-58	28.9	59.9
hIle-59	27.2	45.4
hPro-60	38.1	29.1
hGlu-61	41.4	49.8
hGlu-62	53.6	71.2
hTyr-63	43.5	32.9
hLeu-64	76.4	66.7

[a] The number of contributing atoms is indicated in parentheses.
[b] Unambiguous atomic positions could not be found for the linker hPro-$(hGly)_4$, hAsp-53, hGly-54, hGln-65 or for the side chain of hAsp-55 beyond Cβ.
[c] Cβ only.

binary complex, the side chain of hAsp-55 could not even be located, making it doubtful that it forms a salt bridge in this case. Mutant studies (Table 2) also show that hGlu-57 is the most important of the charged residues in the C-terminal tail of hirudin with Glu-58 being somewhat ambiguous and hAsp-55, hGlu-61, and hGlu-62 considerably less important in binding to thrombin (Betz et al., 1991a; Karshikov et al., 1992), which is in agreement with the structure. In the complex of bovine α-thrombin and hirudin (Vitali et al., 1992) hAsp-55 forms a salt bridge with Arg-73 of thrombin, while hGlu-57 again forms a salt bridge with Arg-75 but not with Arg-77A. The side chains of hGlu-58, hGlu-61, and hGlu-62 do not interact with thrombin. In contrast to the very specific interactions made by hydrophobic residues of the hirudin C-terminal fragment, those of the charged residues vary considerably according to local environment (crystal packing). This supports the idea that the function of the charged residues is to facilitate long-range alignment of the molecules and not for specific, short-range interactions (Karshikov et al., 1992).

Contrary to expectations, the sulfate of hTyr-63 in the ternary complex does not form a salt bridge with thrombin, but rather a very tight network of hydrogen bonds (Fig. 2; Kinemage 1). The only nearby positive charge on thrombin is on the side chain of Lys-81, but its side chain could not be located in the crystal structure, implying either static or dynamic disorder and not a fixed conformation anchored by a salt bridge to the sulfate of hTyr-63. In the structure of Skrzypczak-Jankun et al. (1991), Lys-81 is pointing away from the sulfate group, although its location is reported as being ambiguous. Otherwise, the interactions of the sulfate group with thrombin are similar in the two structures. A large number of hydrophobic interactions between thrombin and hPhe-56, hIle-59, hPro-60, hTyr-63, and hLeu-64 of the C-terminal fragment of hirudin are made upon binding. Numerically, hPhe-56 makes the most contacts with thrombin, and its loss through replacement with alanine causes a 0.45-kcal/mol decrease in the free energy of binding (Betz et al., 1991b). It can be replaced with tyrosine without loss, but tryptophan seems to be too large. Replacement with branched amino acids (Leu, Val, Ile, or Thr) causes an even larger energy loss. In general, replacement of amino acids in the C-terminal tail of hirudin with glycine decreases binding more than replacement by alanine (Yue et al., 1992), probably due to entropic effects from loss of flexibility at the conformationally less restrained glycine upon binding. The largest effect is seen upon replacing hIle-59 with a glycine, although the number of contacts lost is small. This could again be due to both the increased flexibility at a critical point in the hirudin structure where it changes from an extended conformation to a helical one and to the loss of intermolecular interactions between hIle-59 and thrombin. The unsulfated tyrosine at position 63 in hirudin makes only hydrophobic contacts with thrombin, particularly with Ile-82. It can be replaced with a phenylalanine without loss of binding energy. Because hTyr-63 binds with only one face toward thrombin, replacement with branched-chain amino acids (e.g., Val or Leu) does not cause as much disruption as it does for hPhe-56, which binds in a narrow hydrophobic pocket in thrombin. The last hydrophobic residue of hirudin, hLeu-64, makes contact with the hydrophobic part of the side chain of Lys-36. Both the number and strength of its contacts with thrombin seem to be less than other residues, as evidenced by the relatively small loss of binding energy upon replacement with a glycine residue and its high temperature factors in the complex structures. hGln-65 does not seem to be involved in interactions with thrombin and in fact could not be located in the binary complex structure and had very weak electron density for the ternary complex structure. Skrzypczak-Jankun et al. (1991) were missing this residue in both of their complex structures in a monoclinic crystal form and claimed that the loss of its interactions in the unsulfated hTyr-63 C-terminal hirudin fragment is enough to prevent the last five residues (hPro-60–hLeu-64) from binding to thrombin. It should be noted, however, that this residue itself is only poorly ordered in those structures where it is present. In addition, removal of this residue has very little effect on hirudin binding to thrombin (Yue et al., 1992). In our orthorhombic crystal form there is a neighboring thrombin molecule

interacting with hPro-60 and hGlu-61. These interactions may be sufficient to prevent the last five residues of the C-terminal end of hirudin from dissociating from thrombin in the crystals.

The structures of thrombin complexed with hirudin C-terminal fragments both linked and unlinked to active-site inhibitors demonstrate that the mode of binding of the hirudin C-terminus is through both hydrophilic (especially residues hGlu-57 and sulfated hTyr-63) and hydrophobic (residues hPhe-56, hIle-59, and hLeu-64) interactions and remains essentially unchanged whether free or bound to the rest of hirudin or to small active-site inhibitors (Kinemages 1, 2). The structures explain the effects of mutations of the C-terminus of hirudin on binding. It is possible to remove the entire core of hirudin and still retain specific binding to thrombin in the nanomolar range, which is encouraging for the search for low molecular weight specific inhibitors of thrombin.

This work also illustrates the possible effects of crystal packing on the structure of a protein or protein complex solved crystallographically. The interpretation of how important a role the last five residues of the hirudin C-terminal fragment (h61–h65) play depends on the form of the crystal. In the work of Skrzypczak-Jankun et al. (1991), it was concluded that, when unsulfated at Tyr-h63, these residues do not bind to thrombin, while in the crystal form presented here, the presence of a symmetry neighbor gives the appearance of binding of these residues to thrombin. Likewise, whether or not specific side chains of hirudin interact with the thrombin is also dependent on neighboring molecules in the crystal. The interaction of the C-terminal tail of hirudin with thrombin seems especially dependent on crystal-packing effects, especially in the structure of Skrzypczak-Jankun et al. (1991). A second crystal form allows more confidence in the interpretation of the binding; interactions that are the same in different crystal forms are likely to be due to the intrinsic affinity of the two molecules for each other. Effects of crystal contacts can be detected by comparing different crystal forms of similar compounds. This analysis provides a modified picture of binding of the C-terminal tail of hirudin to thrombin compared to that described before. In a similar fashion, the variety of conformations for the autolysis loop (residues 146–150) is an example of the value of the analysis of different crystal forms in the investigation of protein structure–function relationships.

Materials and methods

Synthesis of (D-Phe)-Pro-Arg-Pro-(Gly)$_4$-Asp-Gly-Asp-Phe-Glu-Glu-Ile-Pro-Glu-Glu-Tyr-Leu-Gln (CGP 50,856)

The peptide sequence was synthesized in a stepwise manner on a solid-phase using Fmoc (Carpino & Han, 1970) as a temporary α-amino protecting group and acid-labile side-chain protecting groups—Arg(Pmc), Asp(tBu), Glu(tBu), Tyr(tBu), and Gln(Trt) (Sieber & Riniker, 1991). 4-Alkoxy-benzyl-alcohol polystyrene (cross-linked with 1% DVB) was esterified with Fmoc-Gln(Trt) using the 2,6-dichloro-benzoylchloride method (Sieber, 1987), and amino acid derivatives were activated for coupling with DCCI/HOBt as described by Rink et al. (1989). Repeated washings of the resin were done with DMA and isopropanol. The kinetics of the Fmoc cleavages (20% piperidine in DMA) were monitored as described by Rink and Ernst (1990). Average coupling yields were higher than 99%. The protected peptide was cleaved from the resin with TFA/water/ethanedithiol 93:5:2 (v/v) (10 min), and the protecting groups were removed with the same reagent (60 min) at 25 °C. The peptide was precipitated with DIPE/PE 1:1 (v/v) and dried in vacuo. HPLC purification was performed with 40-mg batches on a Nucleosil 5C18 column (20 × 250 mm), using the following conditions: eluents: A 0.1% TFA/water, B 0.1% TFA/ACN; linear gradient fractions, containing the main peak, were collected, concentrated, and lyophilized. Purity was better than 98% (HPLC). FAB-MS gave a molecular weight of (MH^+) 2,309.9 (expected: 2,310.4).

Crystallization

PPACK and Tyr-63-sulfated hirudin 55–65 were purchased from Bachem (Bubendorf, Switzerland). Human α-thrombin was prepared as described previously (Noé et al., 1988). Thrombin at a concentration of 4 mg/mL was inhibited by adding a 10-fold molar excess of PPACK, then dialyzed against 2 mM morpholinophenyl sulfonic acid buffer, pH 7.0, containing 0.1 M NaCl and 0.05% NaN_3 and concentrated to 6 mg/mL by the use of Centricon 10 tubes (Amicon). A twofold molar excess of Tyr-63-sulfated hirudin$^{55-65}$ dissolved in water was added to form the ternary complex. Crystallization of the complex was achieved by the hanging drop vapor diffusion technique against 0.1 M sodium acetate buffer, pH 4.0, containing between 6 and 12% PEG 6000. Long, thin needles appeared after 2–3 weeks and reached a maximum size of 0.2 × 0.2 × 0.5 mm. The orthorhombic crystals belong to space group $P2_12_12$, with cell edges of a = 80.9 Å, b = 107.5 Å, and c = 45.9 Å, contain one molecule per asymmetric unit, and diffract to a maximum resolution of 2.5 Å.

The complex of human α-thrombin with CGP 50,856 was prepared by adding a fivefold molar excess of CGP 50,856 to human α-thrombin (5 mg/mL) predialyzed against 2 mM morpholinophenyl sulfonic acid buffer, pH 7.0, containing 0.1 M NaCl and 0.05% NaN_3. Crystallization of the complex was achieved by the hanging drop vapor diffusion technique against 0.1 M sodium acetate buffer, pH 4.0–5.0, containing between 6 and 10% PEG 6000. Crystals nearly isomorphous to the ones from the ternary complex were obtained, belonging to space

group $P2_12_12$ and having cell dimensions of $a = 80.5$ Å, $b = 107.1$ Å, and $c = 45.8$ Å and diffracting to 2.2 Å resolution.

Data collection and processing

All X-ray data were collected using a FAST area detector (Enraf Nonius, Delft, The Netherlands). Graphite-monochromatic $Cu_{K\alpha}$ radiation was provided by an FR 571 rotating anode X-ray generator operated at 40 kV and 70 mA with an apparent focal spot of 0.3×0.3 mm^2. Data from one crystal of the ternary complex of PPACK-inhibited thrombin with Tyr-63-sulfated hirudin 55–65 were collected at a crystal-to-detector distance of 70 mm with a swing-out angle of 15°, allowing data collection to a maximal resolution of 2.5 Å. The crystal was rotated about an arbitrary axis for 90° at one orientation and then for 60° after rotation of the axis to 90° in order to collect the "blind" region of reciprocal space. Images with a width of 0.1° were exposed for 120 s. The data were evaluated on-line using the program MADNES (Messerschmidt & Pflugrath, 1987). The 35,785 measured intensities were processed and merged using the CCP4 program package (Daresbury Laboratory) leading to 13,404 unique reflections, corresponding to 93% of all possible unique reflections to 2.5 Å resolution. The merging R-factor (R_{merge}), defined as $\sum(|I - \langle I\rangle|)/\sum I$, is 0.080 for data between 30 and 2.5 Å. In the case of the binary complex of thrombin with the bifunctional inhibitor CGP 50,856, two crystals were used to collect data. The crystal-to-detector distance was 60 mm and the swing-out angle 20°, giving data to a maximal resolution of 2.2 Å. The first crystal was rotated about an axis approximately parallel to the longest dimension of the crystal for 90°, whereas the second crystal was rotated for 30° about an axis perpendicular to this orientation. Frames with a width of 0.1° were taken with an exposure time of 120 s. The 43,768 measurements provided data for 18,572 unique reflections, 89% of the total data set. The R_{merge} is 0.086 for data between 30 and 2.2 Å. The occurrence of screw axes was established by examination of the intensities measured from crystals of both complexes along the h00, 0k0, and 001 axes.

Structure solution

The orientation of thrombin in the unit cell of the crystal of the ternary complex was determined by the fast rotation function (Crowther, 1972) using data between 8.0 Å and 4.0 Å resolution and the refined model of thrombin alone (Bode et al., 1989). Positioning of the thrombin molecule was achieved using the translation function of Crowther and Blow (1967) as implemented in the program TFSGEN. The translation function provided a clear solution when applied in space group $P2_12_12$. A peak (16 rms above the mean) was obtained that was 2.1 times higher than the first noise peak. The translation function applied in related space groups ($P2_12_12_1$ and $P222_1$) gave no clear peak above the noise, confirming the space group as $P2_12_12$, as was determined from the diffraction data. These rotation/translation results were also applied to the PPACK molecule in the original trial structure for an approximate fit. To roughly position the C-terminal fragment of hirudin, the thrombin–hirudin structure (Grütter et al., 1990) was fitted to the new structure on the basis of the thrombin Cα positions alone. Both the PPACK and C-terminal fragments were then precisely positioned using an $F_o - F_c$ difference electron-density map.

The crystals of the binary complex are isomorphous with those of the ternary complex. An $F_o - F_c$ difference electron-density map, where F_c, a_c were calculated from the thrombin molecule alone, was used to fit the bifunctional inhibitor CGP 50,856. No electron density was observed for the Pro-$(Gly)_4$ linker of the inhibitor.

Structure refinement

The structures were refined with the restrained refinement program TNT (Tronrud et al., 1987). For the ternary complex a new dictionary group for PPACK covalently bound to Ser-195 and His-57 of thrombin had to be created as well as a sulfate group attached to a tyrosine for Tyr-63 of the hirudin C-terminal fragment. Molecular dynamics refinement was performed using the program XPLOR (Brünger et al., 1987). The molecule was allowed to equilibrate at 3,000 K for 2,000 cycles of 0.5 fs each, followed by slow cooling to 300 K in 1,000 cycles of 0.5 fs each. Throughout refinement, when local convergence had occurred, visual inspection of electron-density maps and manual correction were performed on an Evans and Sutherland PS-390 computer graphics system using the program FRODO (Jones, 1978). Both omit maps and σ_A maps (Read, 1986) were used. Solvent molecules were located by examination of the highest peaks in $F_o - F_c$ difference maps (cutoff 4.0σ above the mean) with respect to potential hydrogen bond formation with appropriate protein atoms or with previously accepted solvent molecules. Individual isotropic temperature factors were refined for the structure of thrombin complexed with CGP 50,856. Due to the lower resolution of the diffraction data from crystals of thrombin with PPACK and the C-terminal fragment of hirudin (2.5 Å), only group temperature factors, where each residue constituted a group, were refined.

α-Thrombin–PPACK–Tyr-63-sulfated hirudin$^{55-65}$ (ternary complex)

After adding PPACK and the C-terminal fragment, the crystallographic R-factor was 0.432 for all data between 10.0 and 2.5 Å resolution. Six cycles of TNT refinement brought the R-factor down to 0.356 before reaching lo-

cal convergence. Examination of a $2F_o - F_c$ (Read, 1986) electron-density map indicated a few minor manual improvements and that the active-site loop 146–150 possessed a different conformation than that in the thrombin–PPACK complex trial structure. An omit $F_o - F_c$ difference electron-density map, where these residues were omitted from the calculated structure factors, allowed easy interpretation of the correct conformation of this loop. Further restrained least-squares refinement with TNT alternating with molecular dynamics refinement with XPLOR brought the R-factor down to 0.255. Both $F_o - F_c$ and $2F_o - F_c$, σ_A maps were used to make manual corrections and to locate solvent molecules. In addition, strong electron density extending from the side chain of Asn-60G allowed addition of the first carbohydrate moiety, an N-acetyl glucosamine group. Alternating cycles of TNT refinement and manual corrections on the computer graphic system followed by group temperature factor refinement brought the R-factor down to 0.202 for all data between 10.0 and 2.5 Å resolution with good stereochemistry (rms deviation of bond lengths and angles of 0.019 Å and 3.4°, respectively). The final structure consists of 2,311 atoms from thrombin, 30 atoms from PPACK, 104 atoms from the C-terminal fragment of hirudin, and 72 solvent atoms.

α-Thrombin–CGP 50,856 complex (binary complex)

Electron density in the starting $F_o - F_c$ map was quite clear for the first three residues (D-Phe-Pro-Arg) of the inhibitor CGP 50,586, as well as for residues h56–h64, although some fairly large corrections were required for the latter. The starting model of thrombin plus inhibitor gave a crystallographic R-factor of 0.387. Eight cycles of TNT refinement brought this down to 0.316 before molecular dynamic refinement. XPLOR effected only slight improvement in the R-factor, to 0.290, with a large improvement in reducing bad van der Waals contacts and a slight worsening of other stereochemical parameters. Four more cycles of TNT refinement brought the R-factor down to 0.274. Alternating individual temperature factor refinement with positional refinement brought the R-factor down to 0.223 with a concomitant improvement in stereochemistry. An $F_o - F_c$ difference map revealed weak electron density for hAsp-55 of the inhibitor, but no residues further toward the N-terminus could be found. Likewise, no electron density could be found beyond Arg-3, although that for Arg-3 itself is quite clear and unambiguous, implying that the inhibitor had been cleaved. As in the ternary complex, clear electron density extending from the side chain of Asn-60G allowed the addition of one N-acetyl glucosamine group of the carbohydrate moiety (Fig. 9). Solvent molecules were added at this point, excluding any candidates near the missing inhibitor residues. Alternating individual temperature factor and positional refinement with examination of electron-density maps on the computer graphics display resulted in a final crystallographic R-factor of 0.177 for all data between 6.0 and 2.2 Å resolution with good stereochemistry (rms deviation from ideal of bond lengths and angles of 0.014 Å and 3.0°, respectively). The final structure consists of 2,394 atoms from thrombin, 134 atoms from the inhibitor CGP 50,856, and 93 solvent atoms.

In both the ternary and binary complex structures, a number of residues at the termini of the A and B chains of thrombin had weak, ambiguous electron density, presumably due to disorder, and could not be placed with certainty. Residues 1H–1C and 33–36 of the A chain and the last two residues of the B chain could not be located. In addition, the side chains of four lysine residues in thrombin could not be fully located (81, 110, 149E, and 236). The last residue of the C-terminal fragment, hGln-65, also could not be unambiguously located in the binary complex structure. A plot of the main-chain dihedral angles shows only one major violation, that of Phe-7 in the A chain of thrombin (Fig. 10).

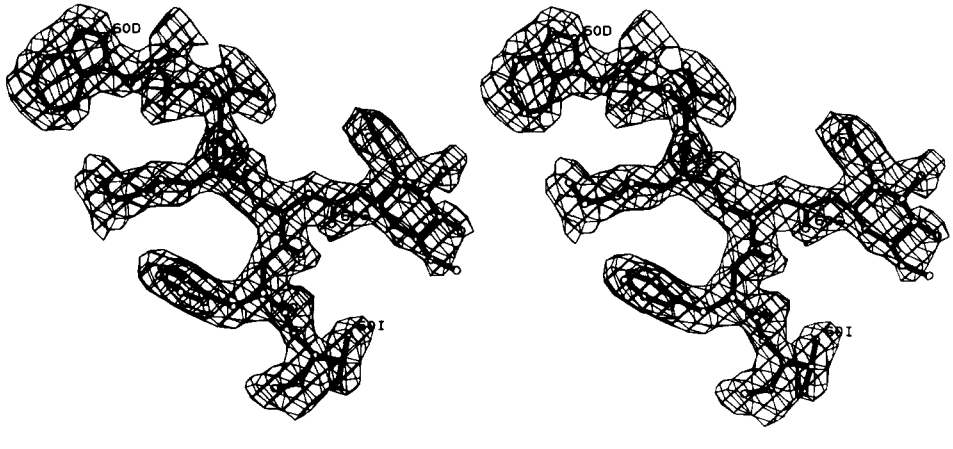

Fig. 9. Electron density for thrombin (striped bonds) complexed with CGP 50,856 around the glycosylation site Asn-60G. The first N-glucosamine unit is shown with solid bonds. The electron density is from a $2F_o - F_c$, σ_A 2.2 Å Fourier map (Read, 1986) and is contoured at 1 rms above the mean.

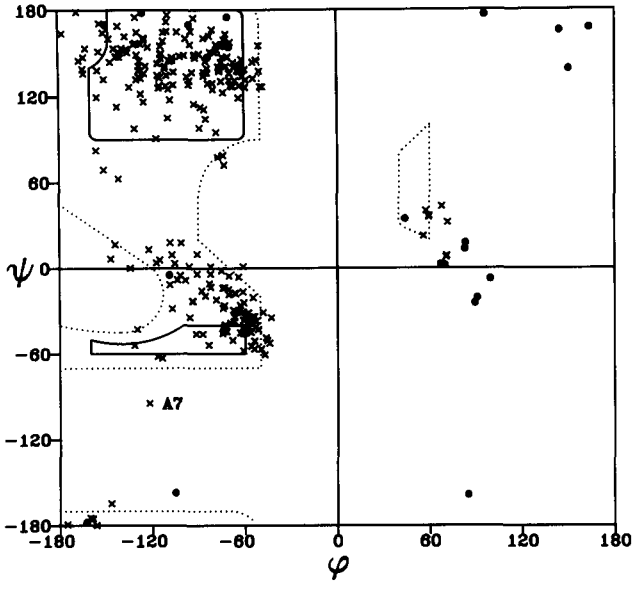

Fig. 10. ϕ, ψ Plot of the main-chain conformational angles of the CGP 50,856-thrombin complex. Glycine residues are shown as dots, other residues as crosses. Only residue 7-Phe of the A chain of thrombin is significantly outside the allowed regions.

Acknowledgments

We thank M. Carvajal for excellent technical assistance, Dr. J. van Oostrum for critically reading of the manuscript, and Dr. Stuart R. Stone for discussions of many aspects of this work.

References

Bagdy, D., Barabas, E., Gráf, L., Petersen, T.E., & Magnusson, S. (1976). Hirudin. *Methods Enzymol. 45*, 669-678.

Banner, D.W. & Hadváry, P. (1991). Crystallographic analysis at 3.0-Å resolution of the binding to human thrombin of four active site-directed inhibitors. *J. Biol. Chem. 266*, 20085-20093.

Betz, A., Hofsteenge, J., & Stone, S.R. (1991a). Ionic interactions in the formation of the thrombin-hirudin complex. *Biochem. J. 275*, 801-803.

Betz, A., Hofsteenge, J., & Stone, S.R. (1991b). Role of interactions involving C-terminal nonpolar residues of hirudin in the formation of the thrombin-hirudin complex. *Biochemistry 30*, 9848-9853.

Bode, W. & Huber, R. (1991). Ligand binding: Proteinase-protein inhibitor interactions. *Curr. Opinion Struct. Biol. 1*, 45-52.

Bode, W., Mayr, I., Baumann, U., Huber, R., Stone, S.R., & Hofsteenge, J. (1989). The refined 1.9 Å crystal structure of human α-thrombin: Interaction with D-Phe-Pro-Arg chloromethylketone and significance of the Tyr-Pro-Pro-Trp insertion segment. *EMBO J. 8*, 3467-3475.

Bode, W., Turk, D., & Karshikov, A. (1992). The refined 1.9-Å X-ray crystal structure of D-Phe-Pro-Arg chloromethylketone-inhibited human α-thrombin: Structural analysis, overall structure, electrostatic properties, detailed active site geometry, and structure-function relationships. *Protein Sci. 1*, 426-471.

Bourdon, P., Jablonski, J.-A., Chao, B.H., & Maraganore, J.M. (1991). Structure-function relationships of hirulog peptide interactions with thrombin. *FEBS Lett. 294*, 163-166.

Braun, P.J., Dennis, S., Hofsteenge, J., & Stone, S.R. (1988). Use of site-directed mutagenesis to investigate the basis for the specificity of hirudin. *Biochemistry 27*, 6517-6522.

Brezniak, D.V., Brower, M.S., Witting, J.I., Walz, D.A., & Fenton, J.W., II. (1990). Human α- to ζ-thrombin cleavage occurs with neutrophil cathepsin G or chymotrypsin while fibrinogen clotting activity is retained. *Biochemistry 29*, 3536-3542.

Brünger, A.T., Kuriyan, J., & Karplus, M. (1987). Crystallographic *R* factor refinement by molecular dynamics. *Science 235*, 458-460.

Carpino, L.A. & Han, G.Y. (1970). The 9-fluorenylmethoxycarbonyl function, a new base-sensitive amino amino-protecting group. *J. Am. Chem. Soc. 92*, 5748-5749.

Clore, G.M., Sukumaran, D.K., Nilges, M., Zarbock, J., & Gronenborn, A.M. (1987). The conformation of hirudin in solution: A study using nuclear magnetic resonance, distance geometry and restrained molecular dynamics. *EMBO J. 6*, 529-537.

Crowther, R.A. (1972). The fast rotation function. In *The Molecular Replacement Method* (Rossmann, M.G., Ed.), pp. 173-178. Gordon and Breach, New York.

Crowther, R.A. & Blow, D.M. (1967). A method of positioning a known molecule in an unknown crystal structure. *Acta Crystallogr. 23*, 544-548.

DiMaio, J., Gibbs, B., Munn, D., Lefebvre, J., Ni, F., & Konishi, Y. (1990). Bifunctional thrombin inhibitors based on the sequence of hirudin. *J. Biol. Chem. 265*, 21698-21703.

Dodt, J., Köhler, S., & Baici, A. (1988). Interaction of site specific hirudin variants with α-thrombin. *FEBS Lett. 229*, 87-90.

Dodt, J., Köhler, S., Schmitz, T., & Wilhelm, B. (1990). Distinct binding sites of Ala^{48}-hirudin$^{1-47}$ and Ala^{48}-hirudin$^{48-65}$ on α-thrombin. *J. Biol. Chem. 265*, 713-718.

Dodt, J., Müller, H.-P., Seemüller, U., & Chang, J.-Y. (1984). The complete amino acid sequence of hirudin, a thrombin specific inhibitor: Application of colour carboxymethylation. *FEBS Lett. 165*, 180-184.

Dodt, J., Seemüller, U., Maschler, R., & Fritz, H. (1985). The complete covalent structure of hirudin. *Biol. Chem. Hoppe-Seyler 366*, 379-385.

Fenton, J.W., II. (1981). Thrombin specificity. *Ann. N.Y. Acad. Sci. 370*, 468-495.

Fenton, J.W., II, Landis, B.H., Walz, D.A., & Finlayson, J.S. (1977). Human thrombins. In *Chemistry and Biology of Thrombin* (Lundblad, R.L., Fenton, J.W., II, & Mann, K.G., Eds.), pp. 43-70. Ann Arbor Science Publishers, Ann Arbor, Michigan.

Folkers, P.J.M., Clore, G.M., Driscoll, P.C., Dodt, J., Köhler, S., & Gronenborn, A.M. (1989). Solution structure of recombinant hirudin and the Lys-47 → Glu mutant: A nuclear magnetic resonance and hybrid distance geometry-dynamical simulated annealing study. *Biochemistry 28*, 2601-2617.

Grütter, M.G., Fendrich, G., Huber, R., & Bode, W. (1988). The 2.5 A X-ray crystal structure of the acid-stable proteinase inhibitor from human mucous secretions analysed in its complex with bovine α-chymotrypsin. *EMBO J. 7*, 345-351.

Grütter, M.G., Priestle, J.P., Rahuel, J., Grossenbacher, H., Bode, W., Hofsteenge, J., & Stone, S.R. (1990) Crystal structure of the thrombin-hirudin complex: A novel mode of serine protease inhibition. *EMBO J. 9*, 2361-2365.

Haruyama, H. & Wüthrich, K. (1989). Conformation of recombinant desulfatohirudin in aqueous solution determined by nuclear magnetic resonance. *Biochemistry 28*, 4301-4312.

Jackson, C.M. & Nemerson, Y. (1980). Blood coagulation. *Annu. Rev. Biochem. 49*, 765-811.

Jones, T.A. (1978). A graphics model building and refinement system for macromolecules. *J. Appl. Crystallogr. 11*, 268-272.

Karshikov, A., Bode, W., Tulinsky, A., & Stone, S.R. (1992). Electrostatic interactions in the association of proteins: An analysis of the thrombin-hirudin complex. *Protein Sci. 1*, 727-735.

Kawabata, S., Morita, T., Iwanaga, S., & Igarashi, H. (1985). Staphylocoagulase-binding region in human prothrombin. *J. Biochem. (Tokyo) 97*, 325-331.

Maraganore, J.M., Bourdon, P., Jablonski, J., Ramachandran, K.L., & Fenton, J.W., II. (1990). Design and characterization of hirulogs: A novel class of bivalent peptide inhibitors of thrombin. *Biochemistry 29*, 7095-7101.

Maraganore, J.M., Chao, B., Joseph, M.L., Jablonski, J., & Ramachandran, K.L. (1989). Anticoagulant activity of synthetic hirudin peptides. *J. Biol. Chem. 264*, 8692-8698.

Markwardt, F. (1970). Hirudin as an inhibitor of thrombin. *Methods Enzymol. 19*, 924-932.

Martin, P.D., Robertson, W., Turk, D., Huber, R., Bode, W., & Edwards, B.F.P. (1992). The structure of residues 7-16 of the Aα-chain

of human fibrinogen bound to bovine thrombin at 2.3-Å resolution. *J. Biol. Chem. 267*, 7911-7920.

Messerschmidt, A. & Pflugrath, J.W. (1987). Crystal orientation and X-ray pattern prediction for area-detector diffractometer systems in macromolecular crystallography. *J. Appl. Crystallogr. 20*, 306-315.

Noé, G., Hofsteenge, J., Rovelli, G., & Stone, S.R. (1988). The use of sequence specific antibodies to identify a secondary binding site in thrombin. *J. Biol. Chem. 263*, 11729-11735.

Qiu, X., Padmanabhan, K.P., Carperos, V.E., Tulinsky, A., Kline, T., Maraganore, J.M., & Fenton, J.W., II. (1992). Structure of the hirulog 3-thrombin complex and nature of the S′ subsites of substrates and inhibitors. *Biochemistry 31*, 11689-11697.

Read, R.J. (1986). Improved Fourier coefficients for maps using phases from partial structures with errors. *Acta Crystallogr. A 42*, 140-149.

Rink, H., Born, W., & Fischer, J.A. (1989). The chemical synthesis of the common-region peptide PAS-57 of the human calcitonin precursor and identification in humans. In *Proceedings of the Eleventh American Peptide Symposium* (Rivier, J.E. & Marshall, G.R., Eds.), pp. 1041-1042. ESCOM Science Publishers, Leiden, The Netherlands.

Rink, H. & Ernst, B. (1990). Glycopeptide solid-phase synthesis with an acidic acid labile trialkoxy-benhydroyl linker. In *Proceedings of the Twenty-First European Peptide Symposium* (Giralt, E. & Andreu, D., Eds.), pp. 418-419. ESCOM Science Publishers, Leiden, The Netherlands.

Rydel, T.J., Ravichandran, K.G., Tulinsky, A., Bode, W., Huber, R., Roitsch, C., & Fenton, J.W., II. (1990). The structure of a complex of recombinant hirudin and human α-thrombin. *Science 249*, 277-280.

Rydel, T.J., Tulinsky, A., Bode, W., & Huber, R. (1991). Refined structure of the hirudin-thrombin complex. *J. Mol. Biol. 221*, 583-601.

Schechter, I. & Berger, A. (1967). On the size of the active site in proteases, I. Papain. *Biochem. Biophys. Res. Commun. 27*, 157-162.

Sieber, P. (1987). An improved method for anchoring of 9-fluorenylmethoxycarbonyl amino acids to 4-alkoxybenzyl alcohol resins. *Tetrahedron Lett. 28*, 6147-6150.

Sieber, P. & Riniker, B. (1991). Protection of carboxamide functions by the trityl residue. Application to peptide synthesis. *Tetrahedron Lett. 32*, 739-742.

Skrzypczak-Jankun, E., Carperos, V.E., Ravichandran, K.G., & Tulinsky, A. (1991). Structure of the hirugen and hirulog complexes of α-thrombin. *J. Mol. Biol. 221*, 1379-1393.

Stone, S.R., Dennis, S., & Hofsteenge, J. (1989). Quantitative evaluation of the contribution of ionic interactions to the formation of the thrombin-hirudin complex. *Biochemistry 28*, 6857-6863.

Stone, S.R. & Hofsteenge, J. (1986). Kinetics of the inhibition of thrombin by hirudin. *Biochemistry 25*, 4622-4628.

Stubbs, M.T., Oschkinat, H., Mayr, I., Huber, R., Angliker, H., Stone, S.R., & Bode, W. (1992). The interaction of thrombin with fibrinogen. *Eur. J. Biochem. 206*, 187-195.

Tronrud, D.E., Ten Eyck, L.F., & Matthews, B.W. (1987). An efficient general-purpose least-squares refinement program for macromolecular structures. *Acta Crystallogr. A 43*, 489-501.

Vitali, J., Martin, P.D., Malkowski, M.G., Robertson, W.D., Lazar, J.B., Winant, R.C., Johnson, P.H., & Edwards, B.F.P. (1992). The structure of a complex of bovine α-thrombin and recombinant hirudin at 2.8-Å resolution. *J. Biol. Chem. 267*, 17670-17678.

Walsmann, P. & Markwardt, F. (1981). Biochemische und pharmakologische Aspekte des Thrombininhibitors Hirudin. *Pharmazie 36*, 653-660.

Yue, S.-Y., DiMaio, J., Szewczuk, Z., Purisima, E.O., Ni, F., & Konishi, Y. (1992). Characterization of the interactions of a bifunctional inhibitor with α-thrombin by molecular modelling and peptide synthesis. *Protein Eng. 5*, 77-85.